

CHEMISTRY

AN ASIAN JOURNAL

www.chemasianj.org

Accepted Article

Title: Surface engineering of ITO Substrate to improve memory performance of asymmetric conjugated molecule with a side chain

Authors: Xiang Hou, Xue-Feng Cheng, Xin Xiao, Jing-Hui He, Qing-Feng Xu, Hua Li, Na-Jun Li, Dong-Yun Chen, and Jian-Mei Lu

This manuscript has been accepted after peer review and appears as an Accepted Article online prior to editing, proofing, and formal publication of the final Version of Record (VoR). This work is currently citable by using the Digital Object Identifier (DOI) given below. The VoR will be published online in Early View as soon as possible and may be different to this Accepted Article as a result of editing. Readers should obtain the VoR from the journal website shown below when it is published to ensure accuracy of information. The authors are responsible for the content of this Accepted Article.

To be cited as: *Chem. Asian J.* 10.1002/asia.201700706

Link to VoR: <http://dx.doi.org/10.1002/asia.201700706>

A Journal of



A sister journal of *Angewandte Chemie*
and *Chemistry* – A European Journal

WILEY-VCH

Surface engineering of ITO Substrate to improve memory performance of asymmetric conjugated molecule with a side chain

Xiang Hou,^[a] Xue-Feng Cheng,^[a] Xin Xiao,^[a] Jing-Hui He,^{*[a]} Qing-Feng Xu,^[a] Hua Li,^[a] Na-Jun Li,^[a] Dong-Yun Chen^[a] and Jian-Mei Lu^{*[a]}

Abstract: Organic multilevel random resistive access memories (RRAMs) of electrode/organic layer/electrode sandwich-like structure suffer from poor reproducibility such as low effective ternary device yield and wide threshold voltage distribution, and the improvement by organic material renovation is rather limited. In contrast, surface engineering of the electrode surfaces rather than molecule design was demonstrated to effectively boost the performance of organic electronics. In this work, we introduce surface engineering into organic multilevel RRAMs to enhance their ternary memory performance. A new asymmetric conjugated molecule containing phenothiazine and malononitrile with a side chain (PTZ-PTZO-CN) was fabricated into indium tin oxide (ITO)/PTZ-PTZO-CN/Al sandwich-like memory device. Modifying the ITO substrate by phosphonic acids (PA) prior to device fabrication increases the ternary device yield (the ratio of effective ternary device) and narrows the threshold voltage distribution. The crystallinity analysis reveals that PTZ-PTZO-CN growing on untreated ITO crystallize into two phases. This crystalline ambiguity was eliminated and the sole crystal phase was obtained as same as in the powder state after surface engineering of ITO. The unified crystal structure and improved grain mosaicity result in the lower threshold voltage and thus higher ternary device yield. Our result demonstrated that PA-modification has also improvement on the memory performance based on the asymmetric conjugated molecule with a side chain.

Introduction

In recent years, the explosive growth of information urges new information storage techniques to catch up the increasing requirement of information density. As a new storage technique, random resistive access memories (RRAM) work on the resistance change of dielectric solid-state material switched by external voltages. RRAMs has faster timescales (switching time < 10 ns),¹ low power consumption,² a simple and small cell

structure and three-dimensional stackability, which are all able to turbo the information density.³ In addition, RRAMs are able to store more than two states per cell (for example, three states), leading to the multilevel (ternary) RRAM, which can further significantly increase the capacity.

Inspired by these advantages, various inorganic,⁴ organic,^{1a, 5} hybrid⁶ and bio-material⁷ systems were exploited as the active materials of multilevel RRAMs. Among them, small conjugated molecule⁸ has garnered scientific interest over the past few years because of their low weights, flexibility, handy process and structural tailorability.^{3, 9} Several important parameters of the devices such as the ternary device yield (the ratio of effective ternary device among a batch of memory cells), threshold voltage, ON/OFF current ratios could be partially improved through molecular design by adjusting the terminal electron acceptors,¹⁰ conjugation length,^{3b, 11} planarity,¹² and side chains¹³ However, recent reviews commented that such improvement is rather limited and not rationalized.^{3a} Therefore, other strategies rather than molecular design to improve RRAM performance are highly desirable.

Indium tin oxide (ITO) glass is widely used as the bottom electrode of organic electronics, including RRAM, organic light emitting diodes (OLEDs) and organic photovoltaics (OPVs). Both surface energy matching and work function compatibility of ITO have important roles in OLED and OPV performance after modification.¹⁴ Recently, we demonstrated that surface engineering of ITO substrates by phosphonic acids (PA) prior to fabrication of organic ternary RRAMs produced the highest ternary device yield and much better reproducibility, because the deposited squaraine molecule (SA-Bu) with symmetrical butyl tail/rigid core/butyl tail crystallize more orderly than on the untreated ITO.¹⁵ To verify the general applicability of PA-modification, conjugated molecules with asymmetric side chain are worthy of testing.

In this paper, a new conjugated molecule containing phenothiazine and malononitrile moiety with asymmetric side chain, namely 2-((7-(4-(10H-phenothiazin-10-yl) phenyl)-10-octyl-5-oxido-10H-phenothiazin-3-yl) methylene) malononitrile (PTZ-PTZO-CN) was designed, synthesized and fabricated into RRAMs on PA-modified ITO. This T-shape molecule has a large conjugated plane ended a loose alkyl chain at the center position (**Figure 2b**). Meanwhile, its malononitrile and sulfoxide groups are demonstrated to promising candidates for memory applications due to their outstanding properties as electron acceptors.¹⁶ Our result demonstrated that PA-modification also has improvement on the memory performance based on conjugated molecule with asymmetric side chain.

[a] X. Hou, X.-F.Cheng, X. Xiao, Prof. J.-H. He, Prof. Q.-F.Xu, Prof. H. Li, Prof. N.-J. Li, Prof. D.-Y.Chen, Prof. J.-M. Lu
College of Chemistry, Chemical Engineering and Materials Science
Collaborative Innovation Center of Suzhou Nano Science and
Technology Institution
Soochow University
Suzhou 215123 (P.R.China)
E-mail: jinghhe@suda.edu.cn
lujm@suda.du.cn

Supporting information for this article is given via a link at the end of the document.

Results and Discussion

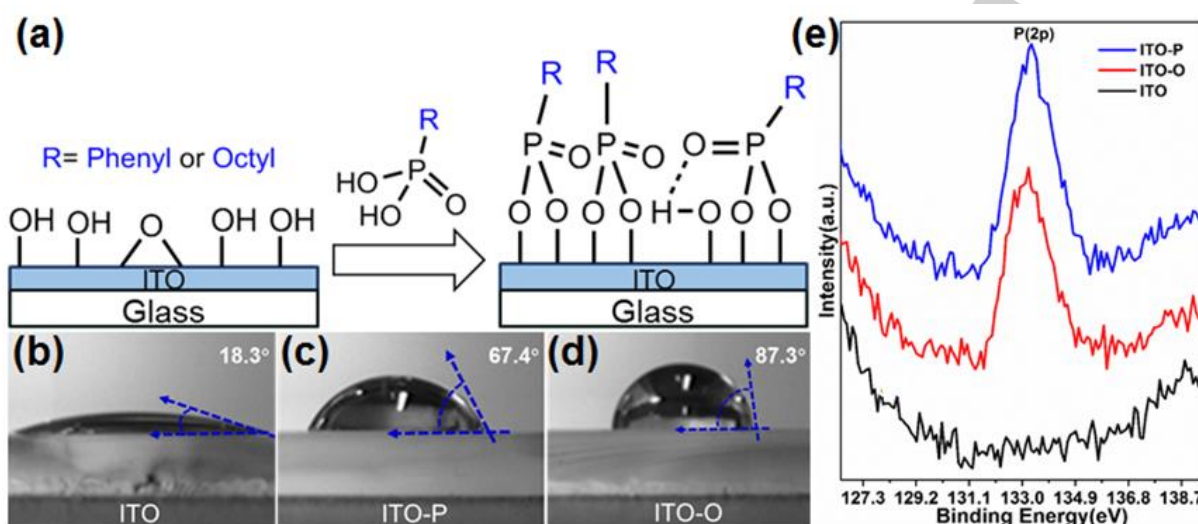


Figure 1. (a) The process of surface modification by phosphonic acids on the surface of ITO glass; (b), (c), (d) The wettability of the test in air; (e) The XPS spectra of P(2p) of PA-modified ITO substrates.

We modified the ITO substrate by PAs self-assembly as shown in **Figure 1a**. To obtain the highest surface coverages of phosphonic acids on ITO surfaces, the tethering by aggregation and growth procedure (T-BAG)¹⁷ was conducted. Two types of ITO substrates were obtained by reacting with phenylphosphonic acid and octylphosphonic acid, named ITO-P, ITO-O, respectively. The surface of the ITO consists of indium tin oxide, hydroxyl and carbonyl, which showed well wettability for the hydrogen bond. The contact angle of ITO is about 18.3°, which corresponds well to the publication. After PAs treatment, the wettability of ITO-P and ITO-O appears 67.4° and 87.3°, respectively (**Figures 1c** and **1d**). This result confirms that the surfaces of ITO-P and ITO-O present a typical hydrophobic property for the octyl group and phenyl on the surface after modification. Hence the change of wettability of these surfaces proves the successful modification of ITO surfaces.

In order to confirm that PAs have been successfully modified to the surface onto substrate, XPS and IR characterization are conducted. The XPS P_{2p} spectra of ITO-P, ITO-O and original ITO are displayed in **Figure 1e**. For ITO-P and ITO-O, the P_{2p} peaks could be appears at about 133.2eV, whereas no distinct feature of the original ITO is observed in this range. This peak position corresponds to the oxidation state of P(V) and in good agreement with the previous study,^{15, 17b} confirming that the existence of PAs(**Figure 1a**). In addition, the IR spectrum of ITO-O (**Figure S1**) showed $\nu_{\text{antisym}} \text{CH}_2 = 2926 \text{ cm}^{-1}$ (indicative of alkyl chain) and $\nu_{2\text{sym}} \text{CH} = 2851 \text{ cm}^{-1}$. 3007 cm^{-1} , $1600\text{--}1450 \text{ cm}^{-1}$ (1604 , 1512 and 1449 cm^{-1}), 768 cm^{-1} , 702 cm^{-1} could be attributed to the characteristic vibration peaks of the benzene ring. These modes strongly imply the existence of PAs.¹⁷

Next, a new conjugated molecule with a side chain, 2-((7-(4-(10H-phenothiazin-10-yl) phenyl)-10-octyl-5-oxido-10H-phenothiazin-3-yl) methylene) malononitrile (PTZ-PTZO-CN) was synthesized and used as the active material in our RRAM

devices. Synthesis of PTZ-PTZO-CN was on the basis of the method as described in literature.¹⁸ The molecular structure of PTZ-PTZO-CN is shown in **Figure 2b** and the detailed synthesis and characterization of PTZ-PTZO-CN are described in the Experimental Section as well as in **Figure S2**. NMR (**Figures S3** and **S4**) and HRMS spectra were measured to ensure that the target molecule is obtained.

The sandwich-structured organic memory devices were fabricated through spin-coating of PTZ-PTZO-CN solutions onto ITO substrates (ITO-O, ITO-P and original ITO), followed by thermal deposition of Al electrodes as shown in **Figure 2a**. The film thickness of the organic active layer and Al electrode are both about 100 nm (**Figure 2c**). All the memory devices exhibit binary and ternary Write-Once-Read-Many Times (WORM) memory behaviors. The typical electrical switching and memory effects of the binary (**Figure 2d**) and ternary devices (**Figure 2e**) were revealed respectively by I-V characteristics. A voltage sweep was applied from 0 to -6.0 V, and the compliance current was set at 0.1 A. For the binary property, the device was initially in the low conductive ("0" or OFF) state. The current of the device increases slowly as the applied voltage increased, until the voltage reaches -1.85 V and the current abruptly jumps to 10^{-2} A, which indicated the device transition from the low conductive ("0" or OFF) state to the high conductive ("1" or ON) state. Then the device retained its high conductive state in the subsequent forward and reverse biased sweeps with bias up to $\pm 6\text{V}$, suggesting the devices showing the binary WORM electric memory characteristics (**Figure 2d**).

Rather than one jump, two abrupt jumps were observed at -1.1 and -2.7 V on a ternary device (in **Figure 2e**), when the voltage was sweated from 0 to -6 V to. The current ratio of these three states is $1:10^2:10^5$, indicating a transition from the low-conductive (OFF) state to an intermediate-conductive (ON1) state, then to a highly conductive (ON2) state. These OFF to

For internal use, please do not delete. Submitted_Manuscript

ON1 and ON1 to ON2 transitions could be considered as “writing” processes in memory operation (**Sweep 1**). The ON2 state was also maintainable during negative sweeps from 0 to -6.0 V (**Sweep 2**) and positive sweeps from 0 to 6.0 V (**Sweep 3**). When a lower negative voltage was applied from 0 to -3 V to another cell of the device, the OFF-to-ON1 transition occurs at about -1.1V (**Sweep 4**). Furthermore, the ON1-to-ON2 transition occurs in the same cell at -2.7 V by **Sweep 5**. Finally, this ON2 state could be sustainable during the negative and positive sweeps (**Sweeps 6 and 7**), which indicate the devices showing

the ternary WORM electric memory characteristics, of potential application in archive storage.^{3a, 5b, 19} For the devices with WORM property, the stability of the devices was evaluated. The retention time tests were performed under a constant stress of -0.8 V for the ON or OFF states of the binary devices (**Figure 2f**) and the ON2, ON1 or OFF states of the ternary devices (**Figure 2g**). The ON/OFF current ratios could be maintained and no obvious degradation in current was observed after a testing period of 6000 s.

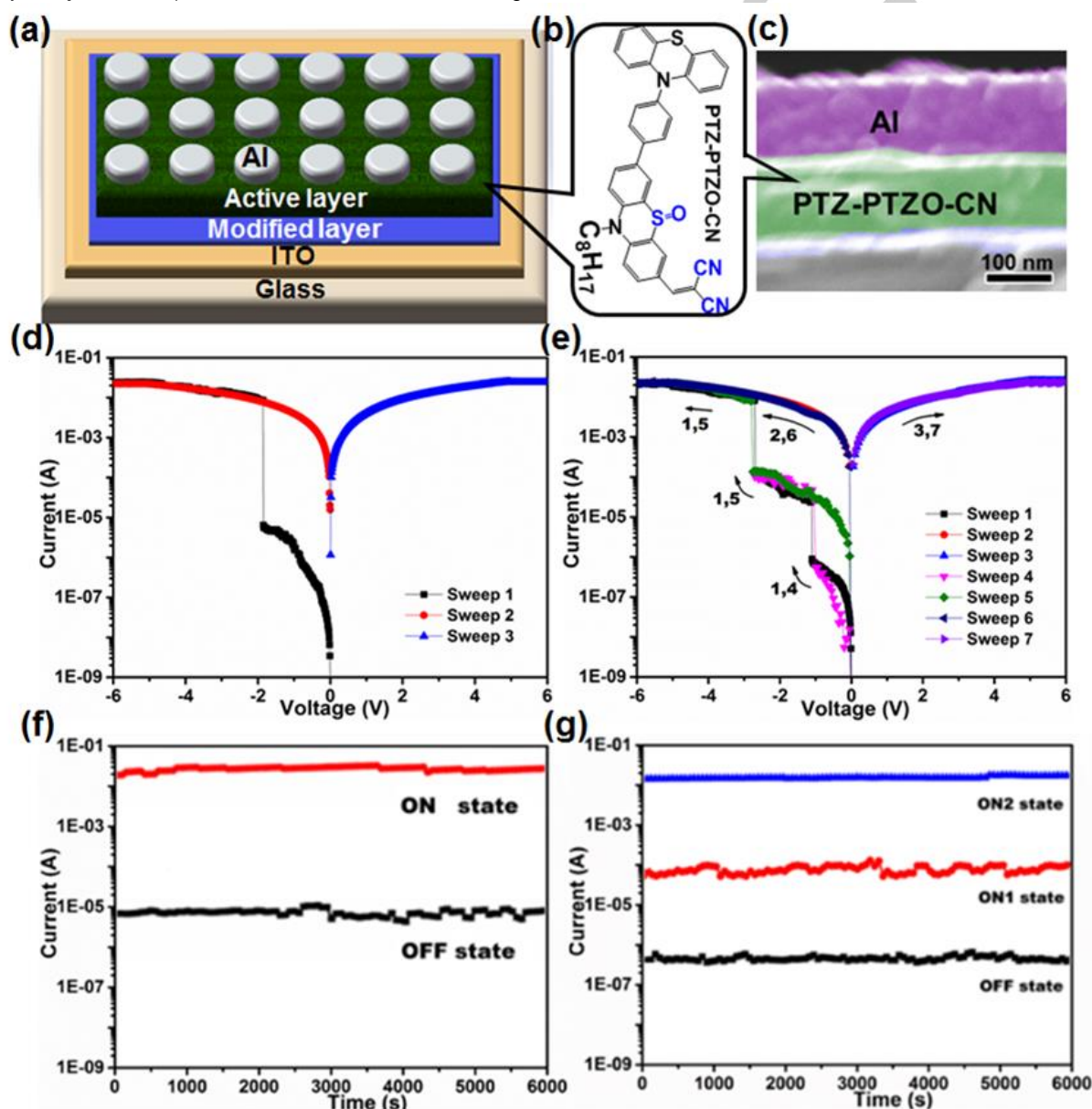


Figure 2. (a) The Diagram of the prototype sandwich device; (b) Molecular structure of PTZ-PTZO-CN; (c) SEM images of a cross-section view of the fabricated RRAM devices; Typical Current-voltage (I–V) characteristics of the binary devices(d) and ternary devices(e). Characteristic retention stability of PTZ-PTZO-CN based memory devices ((f) binary and (g) ternary) measured under a constant stress of -0.8 V at room temperature.

Although both binary and ternary memory switching are observable on all three types of ITO substrates, the ratio of effective ternary device (ternary device yield) and threshold voltages are improved by PA-modification. As shown in **Figure 3**,

For internal use, please do not delete. Submitted_Manuscript

150 cells were tested and the ternary yield on original ITO is as low as 28%. After surface modification, the ratios raise to 38% (for ITO-P) and 40% (for ITO-O), respectively.

The switching threshold voltages (V_{thS}) distributions also reflected the improvement of the device performance after modification. The averaged first (V_{th1}) and second threshold voltages (V_{th2}) of original-ITO devices are -3.40 V and -4.80 V, respectively. After modification, both V_{th1} and V_{th2} of the devices decrease progressively (-2.70/-4.80 V for ITO-P and -2.40/-3.60 V for ITO-O), as shown in **Figure 3**. Moreover, the distribution histograms of the V_{th1} and V_{th2} were shown in **Figure S5**. Compared to ITO and ITO-P, the V_{th1} of the devices based on ITO-O showed a narrower distribution, implying better reproducibility, which is a critical parameter for future application of memory devices.

The above memory performance could be understood firstly from the unique electronic properties of PTZ-PTZO-CN.

According to the cyclic voltammetry (CV) spectra (**Figure S6b**), the HOMO/LUMO values were determined to be -5.02/-2.97 eV. The UV-visible absorption spectra were conducted to study the optical properties of PTZ-PTZO-CN in solution and thin film (**Figure S6a**). The maximum absorption peaks of the compounds in CH_2Cl_2 and in film are at 424 nm and 442 nm, respectively. The peak in the solution could be assigned to the $\pi-\pi^*$ transition within the molecular backbone.²⁰ In comparison, the absorption peak in the film state shows shoulder peaks and a 18 nm bathochromic shift, which indicates that the molecules adopted a more regular arrangement or aggregation in the film,²¹ favoring the charge carrier transport between neighboring molecules in the film. In addition, the onset of UV-absorbance is 604 nm, corresponding to an optical band gap of 2.05 eV. The small band gap and proper HOMO/LUMO position, allowing facile charge injection and carrier transport, which are necessary condition for memory switching.

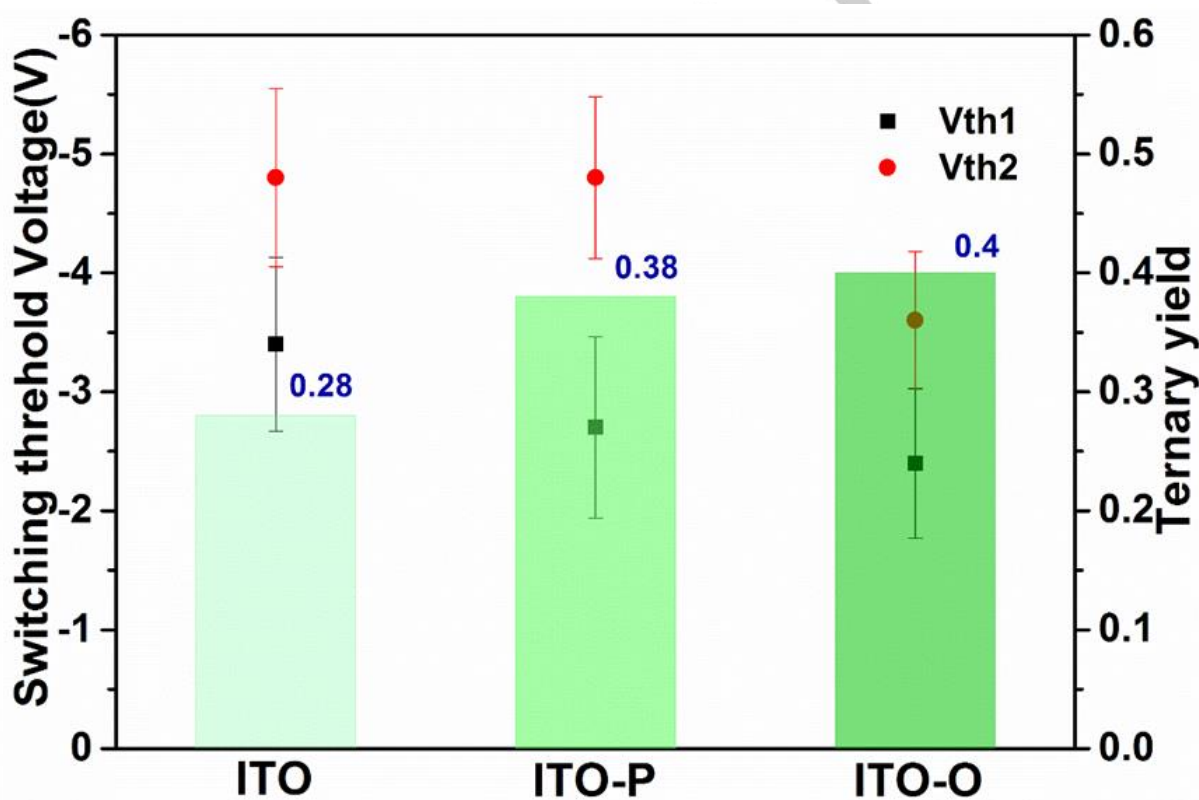


Figure 3. The ternary yield and switching threshold voltages states of memory devices based on three types of substrates.

The intermolecular interaction partially revealed by the above UV-vis spectra is believed to be a key factor to the memory performance, which has been effectively tuned through PA-modification in this work. **Figures 4** and **S7** show the X-ray diffraction patterns of the molecular powder and all three films on ITO, ITO-P and ITO-O. In the powder state, there are several intensive features as well as their higher order diffractions, such as the peak at $2\theta=5.00/10.00/15.25/20.06^\circ$ ($d=17.69/8.89/5.81/4.43$ Å), $2\theta=8.27/16.58^\circ$ ($d=10.68/5.39$ Å) and $2\theta=12.11/24.38^\circ$ ($d=7.31/3.65$ Å). Compared to the powder state, most of peaks fade away and all three films only show two

or three distinct peaks, indicating the crystalline preference in several directions in the films induced by the substrate (**Figures 4a** and **4b**). Particularly, on ITO substrate, three distinct peaks are observable (**Figure 4b**). The first two peaks at $2\theta = 5.02^\circ$ ($d=17.61$ Å) and its second order position 10.04° ($d=8.81$ Å) match well with the powder's pattern. However, the last peak at 11.67° ($d=7.58$ Å) is not found from the powder. On ITO-P substrate, these three peaks also exist, but the last peak at 11.67° become much weaker. In contrast, the film on ITO-O substrate has left only the first two features without the third peak. This discrepancy strong indicates that the third, which is

For internal use, please do not delete. Submitted_Manuscript

not found in the power state, is from an exotic crystal structure different from the powder.

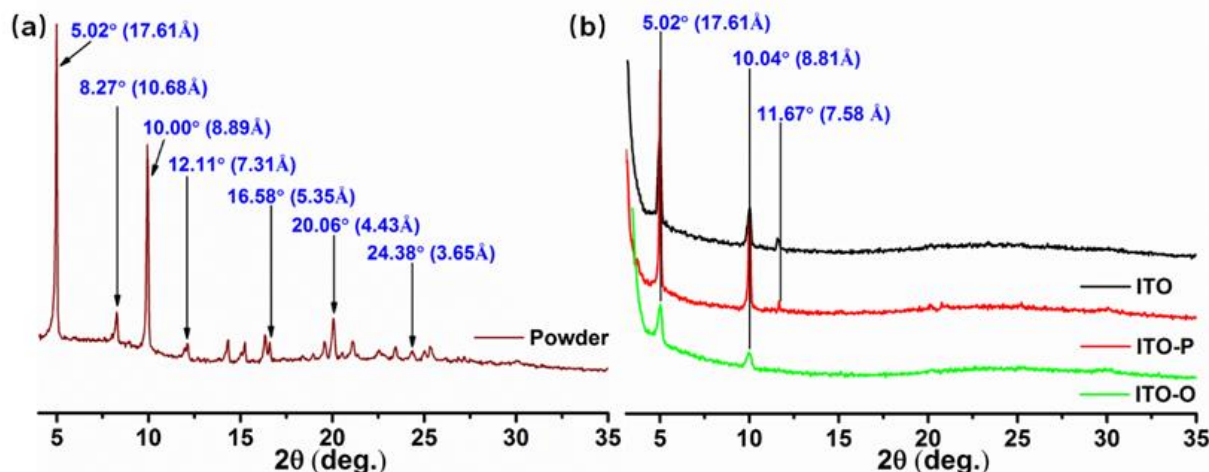


Figure 4. (a) XRD patterns of PTZ-PTZO-CN powder; (b) XRD patterns of PTZ-PTZO-CN films on ITO substrates, ITO-P substrates and ITO-O substrates.

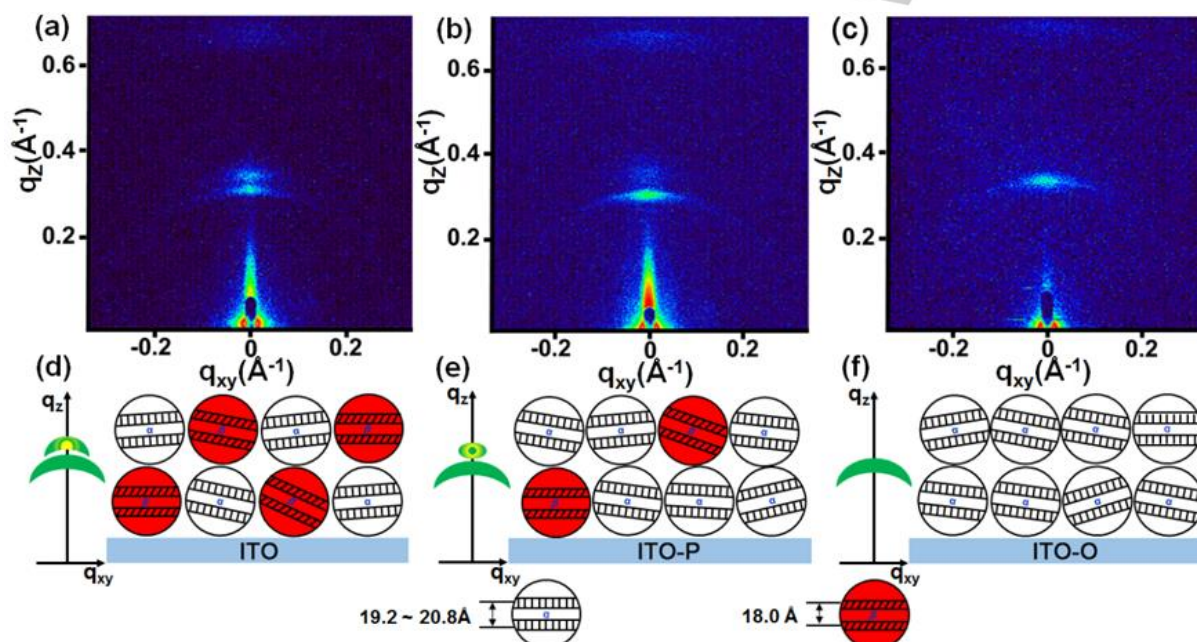


Figure 5. (a), (b), (c) GISAXS patterns and the illustration of the PTZ-PTZO-CN film ((d), (e) and (f)) on ITO, ITO-P and ITO-O substrates, respectively.

We employ grazing-incidence small-angle X-ray scattering (GISAXS) analysis to resolve more details about these two crystalline phases which may be blurred in the small angle range in XRD patterns. In **Figures 5a, 5b, 5c** and **S8**, short arcs sit on the q_z axis, confirming that all grains prefer to aggregate in an out-of-plane preference, in accordance with our interpretation on XRD pattern.²² On original ITO, three short arcs were shown in **Figures 5a** and **5d**, implying spacing distances of 19.8/17.95/9.5 Å ($q_z = 0.32/0.35/0.66 \text{ \AA}^{-1}$). These three arcs correspond to the first two peaks in XRD (19.25 Å/9.17 Å), while the first two arcs (19.8/17.95 Å) are in fact indistinguishable and merge into one peak at $d=19.25 \text{ \AA}$ in XRD. Similarly, the film on ITO-P substrate also has three arcs. However, the intensity of the second arcs

($d=17.9 \text{ \AA}$) is much lower (in **Figures 5b** and **5e**). This peak finally disappears on ITO-O substrate, leaving only the first and third peaks with $d=19.3/9.3 \text{ \AA}$ ($q_z=0.33/0.68 \text{ \AA}^{-1}$) despite of trivial discrepancies. Since the first and second lattice spacing (19.8 and 17.9 Å) in GISAXS pattern, are quite close and larger than the length of the molecule (about 17.3 Å in **Figure S9**), it is further proved that these two spacing unlikely originate from the same crystal phase.

In short, the films on ITO and ITO-P substrates have one more arc at ($d=17.9 \text{ \AA}$) in GISAXS an exotic XRD peak at $2\theta=11.4^\circ$ ($d=7.75 \text{ \AA}$) than on ITO-P substrate or the powder. The plausible explanation is that two crystal phases (structures) of the only molecule exist in the films on ITO and ITO-P substrate, while the

For internal use, please do not delete. Submitted_Manuscript

similarly two crystal phases were also found in our previous study¹⁵ (Figure 5d). After modification by phenylphosphonic acid, the minor phase was gradually suppressed (Figure 5e) and octylphosphonic acid modification can totally eliminate the minor crystal phase (Figure 5f). Therefore, the degree of crystallite ordering is promoted by unifying the crystal phases from two to one, and to highly ordered, lamellar alignment. We suspected that the exotic crystal phase originates from a few layer on the ITO surface, which need to be verified in future but out of scope of this work.

For organic ternary memory, charge-trapping mechanism is widely invoked to explain the resistance switching. In the previous work, we adapted the charge-trapping mechanism²³ to considering the hopping manner of charge transportation in organic film.²⁴ Briefly, a charge in organic film will polarize the surrounding molecules due to the small dielectric coefficient of organic materials. The surrounding will be more conductive, and in turn allowing more charge to be injected in a positive feedback effect.^{8a, 24} This finally creates a conductive channel and cause a resistance abrupt switch. Caused by the positive feedback effect, these channels generally are filamentary and appear with random radius and locations, rather a uniform dispersion on the cross-section as large as the electrode area. The threshold voltages for onset these channels are not an identical value, but of a certain distribution. Nevertheless, more uniform crystal phase and higher lamellar alignment, the conductive channels will be easier to create due to the polarization. Therefore, the switching will occur at a lower electric field (lower external voltages). In consequence, more ternary switching will be found within a constant voltage (0 to -6 V). This explain while device on ITO-O substrate has higher ternary yield if compared to that of ITO and ITO-P substrates. Meanwhile, a uniform crystallinity limit the switching distributed in a narrower range, as we found in Figure 3.

Conclusions

In summary, we demonstrated that surface engineering of indium tin oxide electrode is an effective strategy to improve the performance of organic multilevel RRAMs. Surface engineering of the ITO electrode by phosphonic acids (PA) is feasible to conduct in a solution process and may work cooperatively with other techniques such as molecular design. In this work, an asymmetric and conjugated molecule grown on original ITO crystalizes into two phases. Upon coverage of phenyl and octyl moiety on ITO substrate, this molecule grows in only one crystal structure. The unified crystallinity lowers down the necessary voltage to onset the resistance switching, increasing the final ternary device yield and narrowing the threshold voltage distribution. Our results upgrade the understanding of how intermolecular stacking affects the property of organic RRAMs and reveal an effective strategy to achieve high-performing organic memory devices.

Experimental Section

For internal use, please do not delete. Submitted_Manuscript

Materials

Octylphosphonic acid, phenylphosphonic acid, phenothiazine, p-bromiodobenzene, bis(pinacolato)diboron, 1-bromooctane, 2-Pd(dppf)Cl₂ and Tertrakispalladium were all purchased from commercial sources (TCI, Alfa Aesar, and Sigma-Aldrich). 1,4-dioxane, ethanol and acetone were all purchased from Sinopharm Chemical Reagent Co., Ltd., and used as received without further purification.

Synthesis

The detailed synthesis steps of PTZ-PTZO-CN are described in supporting information.

Modification of ITO Surface with Phosphonic Acids

The ITO glasses of 2 cm × 2 cm size were washed with deionized water, acetone and ethanol in ultrasonic 20 min, respectively. Then, these glasses were dried with nitrogen gun. We use the following modification steps: ITO glasses were placed horizontally on the sample holder, immersed in 1 mmol / L phosphonic acids /tetrahydrofuran solution. The surface of ITO glasses was submerged completely and placed in flowing nitrogen. The solvent was evaporated, until the solution level to drop below the upper surface of ITO in 30 °C. The treated ITO glasses were cleaned with ethanol in ultrasonic and then annealed to 80 °C in nitrogen. After 48 h, ITO glasses were washed with anhydrous ethanol, trimethylamine/ethanol (5% by volume) and ethanol in ultrasonic 20 min, respectively.

Fabrication of the Memory Device

The modified ITO glass substrates (2 cm × 2 cm) were transferred to the glove box, in where moisture content and oxygen levels are less than 1 ppm. The organic layer was vacuum-deposited under a pressure of around 8.0×10^{-6} Torr and the thickness was 100 nm. The aluminum electrodes (0.0314 mm²) were vacuum-deposited at 5.0×10^{-6} Torr through a shadow mask to form top electrodes and the thickness was 100 nm. Both of the thickness was estimated from the SEM images.

Acknowledgements

This work was financially supported by the NSF of China (21336005, 21603158), the major research project of Jiangsu Province office of Education (15KJA150008), Chinese-Singapore Joint Project (2012DFG41900), Suzhou Science and Technology Bureau Project (SYG201524) and the Priority Academic Program Development of Jiangsu Higher Education Institutions (PAPD).

Keywords: Ternary • phosphonic acid • Surface engineering • ITO • Resistive random access memory

- [1] a) J. Ouyang, C.-W. Chu, C. R. Szmada, L. Ma, Y. Yang, *Nat. Mater.* **2004**, 3, 918-922; b) T. Furukawa, *Adv. Colloid. Interface. Sci.* **1997**, 71-2, 183-208.
- [2] a) T. D. Tsai, J. W. Chang, T. C. Wen, T. F. Guo, *Adv. Funct. Mater.* **2013**, 23, 4206-4214; b) S. T. Han, Y. Zhou, C. Wang, L. He, W. Zhang,

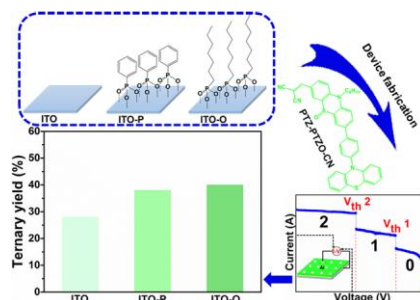
- V. Roy, *Adv. Mater.* **2013**, *25*, 872-877; c) T. Sekitani, T. Yokota, U. Zschieschang, H. Klauk, S. Bauer, K. Takeuchi, M. Takamiya, T. Sakurai, T. Someya, *Science* **2009**, *326*, 1516-1519.
- [3] a) J. C. Scott, L. D. Bozano, *Adv. Mater.* **2007**, *19*, 1452-1463; b) C.-C. Shih, W.-Y. Lee, W.-C. Chen, *Mater. Horiz.* **2016**, *3*, 294-308.
- [4] a) G. Wang, Y. Yang, J.-H. Lee, V. Abramova, H. Fei, G. Ruan, E. L. Thomas, J. M. Tour, *Nano. Lett.* **2014**, *14*, 4694-4699; b) J. Shang, G. Liu, H. Yang, X. Zhu, X. Chen, H. Tan, B. Hu, L. Pan, W. Xue, R. W. Li, *Adv. Funct. Mater.* **2014**, *24*, 2171-2179; c) Y. C. Bae, A. R. Lee, J. B. Lee, J. H. Koo, K. C. Kwon, J. G. Park, H. S. Im, J. P. Hong, *Adv. Funct. Mater.* **2012**, *22*, 709-716.
- [5] a) L.-H. Xie, Q.-D. Ling, X.-Y. Hou, W. Huang, *J. Am. Chem. Soc.* **2008**, *130*, 2120-2121; b) S. Möller, C. Perlov, W. Jackson, C. Taussig, S. R. Forrest, *Nature* **2003**, *426*, 166-169; c) Q.-D. Ling, F.-C. Chang, Y. Song, C.-X. Zhu, D.-J. Liaw, D. S.-H. Chan, E.-T. Kang, K.-G. Neoh, *J. Am. Chem. Soc.* **2006**, *128*, 8732-8733; d) G. Li, K. Zheng, C. Wang, K. S. Leck, F. Hu, X. W. Sun, Q. Zhang, *ACS Appl. Mater. Interfaces* **2013**, *5*, 6458-6462; e) P.-Y. Gu, J. Gao, C.-J. Lu, W. Chen, C. Wang, G. Li, F. Zhou, Q.-F. Xu, J.-M. Lu, Q. Zhang, *Mater. Horiz.* **2014**, *1*, 446-451; f) P.-Y. Gu, F. Zhou, J. Gao, G. Li, C. Wang, Q.-F. Xu, Q. Zhang, J.-M. Lu, *J. Am. Chem. Soc.* **2013**, *135*, 14086-14089.
- [6] a) X. D. Zhuang, Y. Chen, G. Liu, P. P. Li, C. X. Zhu, E. T. Kang, K. G. Noeh, B. Zhang, J. H. Zhu, Y. X. Li, *Adv. Mater.* **2010**, *22*, 1731-1735; b) T. W. Kim, Y. Yang, F. Li, W. L. Kwan, *NPG Asia Mater.* **2012**, *4*, e18; c) B. Hu, C. Wang, J. Wang, J. Gao, K. Wang, J. Wu, G. Zhang, W. Cheng, B. Venkateswarlu, M. Wang, *Chem Sci.* **2014**, *5*, 3404-3408.
- [7] T.-T. Huang, C.-L. Tsai, S. Tateyama, T. Kaneko, G.-S. Liou, *Nanoscale* **2016**, *8*, 12793-12802.
- [8] a) X. F. Cheng, E. B. Shi, X. Hou, S. G. Xia, J. H. He, Q. F. Xu, H. Li, N. J. Li, D. Y. Chen, J. M. Lu, *Chem.-Asian J.* **2017**, *12*, 45-51; b) H. Li, Q. Xu, N. Li, R. Sun, J. Ge, J. Lu, H. Gu, F. Yan, *J. Am. Chem. Soc.* **2010**, *132*, 5542-5543.
- [9] S. T. Han, Y. Zhou, V. Roy, *Adv. Mater.* **2013**, *25*, 5425-5449.
- [10] Q. Zhang, J. He, H. Zhuang, H. Li, N. Li, Q. Xu, D. Chen, J. Lu, *Adv. Funct. Mater.* **2016**, *26*, 146-154.
- [11] J.-C. Hsu, W.-Y. Lee, H.-C. Wu, K. Sugiyama, A. Hirao, W.-C. Chen, *J. Mater. Chem.* **2012**, *22*, 5820-5827.
- [12] a) Y. Li, H. Li, J. He, Q. Xu, N. Li, D. Chen, J. Lu, *Chem.-Asian J.* **2016**, *11*, 906-914; b) X. F. Cheng, E. B. Shi, X. Hou, J. Shu, J. H. He, H. Li, Q. F. Xu, N. J. Li, D. Y. Chen, J. M. Lu, *Adv. Electron. Mater.* **2017**, doi:10.1002/aeml.201700107.
- [13] Q. J. Zhang, J. H. He, H. Zhuang, H. Li, N. J. Li, Q. F. Xu, D. Y. Chen, J. M. Lu, *Chem.-Asian J.* **2016**, *11*, 1624-1630.
- [14] a) E. L. Hanson, J. Guo, N. Koch, J. Schwartz, S. L. Bernasek, *J. Am. Chem. Soc.* **2005**, *127*, 10058-10062; b) P. J. Hotchkiss, H. Li, P. B. Paramonov, S. A. Paniagua, S. C. Jones, N. R. Armstrong, J. L. Brédas, S. R. Marder, *Adv. Mater.* **2009**, *21*, 4496-4501.
- [15] X. Hou, X. Xiao, Q.-H. Zhou, X.-F. Cheng, J.-H. He, Q.-F. Xu, H. Li, N.-J. Li, D.-Y. Chen, J.-M. Lu, *Chem. Sci.* **2017**, *8*, 2344-2351.
- [16] a) Z. Liu, E. Shi, Y. Wan, N. Li, D. Chen, Q. Xu, H. Li, J. Lu, K. Zhang, L. Wang, *J. Mater. Chem. C.* **2015**, *3*, 2033-2039; b) H. Liu, H. Zhuang, H. Li, J. Lu, L. Wang, *Phys. Chem. Chem. Phys.* **2014**, *16*, 17125-17132; c) M.-H. Jung, K. H. Song, K. C. Ko, J. Y. Lee, H. Lee, *J. Mater. Chem.* **2010**, *20*, 8016-8020.
- [17] a) E. L. Hanson, J. Schwartz, B. Nickel, N. Koch, M. F. Danisman, *J. Am. Chem. Soc.* **2003**, *125*, 16074-16080; b) S. A. Paniagua, P. J. Hotchkiss, S. C. Jones, S. R. Marder, A. Mudalige, F. S. Marrikar, J. E. Pemberton, N. R. Armstrong, *The J. Phys. Chem. C.* **2008**, *112*, 7809-7817.
- [18] a) A. Liang, Y. Wang, Y. Liu, H. Tan, Y. Cao, L. Li, X. Li, W. Ma, M. Zhu, W. Zhu, *Chin. J. Chem.* **2010**, *28*, 2455-2462; b) M. A. Reddy, A. Thomas, G. Malleshm, B. Sridhar, V. J. Rao, K. Bhanuprakash, *Tetrahedron Lett.* **2011**, *52*, 6942-6947; c) Y. Wu, H. Guo, J. Shao, X. Zhang, S. Ji, J. Zhao, *J. Fluoresc.* **2011**, *21*, 1143-1154; d) H.-Y. Wang, J.-J. Shi, C. Wang, X.-X. Zhang, Y. Wan, H. Wu, *Dyes. Pigments.* **2012**, *95*, 268-274.
- [19] J. Lin, D. Ma, *J. Appl. Phys.* **2008**, *103*, 024507.
- [20] a) M. Surin, P. Sonar, A. C. Grimsdale, K. Mullen, S. De Feyter, S. Habuchi, S. Sarzi, E. Braeken, A. V. Heyen, M. Van Der Auweraer, F. C. De Schryver, M. Cavallini, J.-F. Moulin, F. Biscarini, C. Femoni, R. Lazzaroni, P. Leclere, *J. Mater. Chem.* **2007**, *17*, 728-735; b) R. D. Schmidt, J. H. Oh, Y.-S. Sun, M. Deppisch, A.-M. Krause, K. Radacki, H. Braunschweig, M. KöNemann, P. Erk, Z. Bao, *J. Am. Chem. Soc.* **2009**, *131*, 6215-6228.
- [21] a) H. Menzel, B. Weichart, A. Schmidt, S. Paul, W. Knoll, J. Stumpe, T. Fischer, *Langmuir.* **1994**, *10*, 1926-1933; b) S. O. Kim, T. K. An, J. Chen, I. Kang, S. H. Kang, D. S. Chung, C. E. Park, Y. H. Kim, S. K. Kwon, *Adv. Funct. Mater.* **2011**, *21*, 1616-1623.
- [22] a) X. H. Cheng, M. K. Das, S. Diele, C. Tschierske, *Angew. Chem. Int. Ed.* **2002**, *41*, 4031-4035; b) F. Liu, M. Prehm, X. Zeng, G. Ungar, C. Tschierske, *Angew. Chem. Int. Ed.* **2011**, *50*, 10599-10602; c) J. Rivnay, S. C. Mannsfeld, C. E. Miller, A. Salleo, M. F. Toney, *Chem. Rev.* **2012**, *112*, 5488-5519; d) M. A. Chavis, D. M. Smilgies, U. B. Wiesner, C. K. Ober, *Adv. Funct. Mater.* **2015**, *25*, 3057-3065; e) E. A. Gaulding, B. T. Diroll, E. Goodwin, Z. J. Vrtis, C. R. Kagan, C. B. Murray, *Adv. Mater.* **2015**, *27*, 2846-2851; f) K.-C. Kao, C.-H. Lin, T.-Y. Chen, Y.-H. Liu, C.-Y. Mou, *J. Am. Chem. Soc.* **2015**, *137*, 3779-3782.
- [23] a) A. Rose, *Phys. Rev.* **1955**, *97*, 1538; b) M. A. Lampert, *Phys. Rev.* **1956**, *103*, 1648-1656.
- [24] Y. Li, H. Li, J. He, Q. Xu, N. Li, D. Chen, J. Lu, *Chem.-Asian J.* **2016**, *11*, 906-914.

Entry for the Table of Contents (Please choose one layout)

Layout 1:

FULL PAPER

Organic molecule was fabricated onto the ITO substrate which was modified by phosphonic acid. These as-fabricated devices perform better memory behaviors, such as higher ternary device yield and lower threshold voltage, compared with those fabricated on unmodified ITO substrate.



Xiang Hou,^[a] Xue-Feng Cheng,^[a] Xin Xiao,^[a] Jing-Hui He,^{*[a]} Qing-Feng Xu,^[a] Hua Li,^[a] Na-Jun Li,^[a] Dong-Yun Chen^[a] and Jian-Mei Lu^{*[a]}

Page No. – Page No.

Surface engineering of ITO substrate to improve memory performance of asymmetric conjugated molecule with a side chain